Proc. Natl. Acad. Sci. USA
Vol. 95, pp. 3257–3262, March 1998
Neurobiology

mRNAs coding for neurotransmitter receptors and voltage-gated sodium channels in the adult rabbit visual cortex after monocular deafferentiation

QUOC-THANG NGUYEN*, CARLOS MATUTE†, AND RICARDO MILEDI*‡

*Laboratory of Cellular and Molecular Neurobiology, Department of Psychobiology, University of California, Irvine, CA 92697-4550; and †Universidad del Pais Vasco, Leioa, Spain

Contributed by Ricardo Miledi, December 31, 1997

ABSTRACT **It has been postulated that, in the adult visual cortex, visual inputs modulate levels of mRNAs coding for neurotransmitter receptors in an activity-dependent manner. To investigate this possibility, we performed a monocular enucleation in adult rabbits and, 15 days later, collected their left and right visual cortices. Levels of mRNAs coding for voltage-activated sodium channels, and for receptors for kainate/α-amino-3-hydroxy-5-methylisoxazole-4-propionic acid (AMPA), *N*-methyl-D-aspartate (NMDA), γ-aminobutyric acid (GABA), and glycine were semiquantitatively estimated in the visual cortices ipsilateral and contralateral to the lesion by the *Xenopus* oocyte/voltage-clamp expression system. This technique also allowed us to study some of the pharmacological and physiological properties of the channels and receptors expressed in the oocytes. In cells injected with mRNA from left or right cortices of monocularly enucleated and control animals, the amplitudes of currents elicited by kainate or AMPA, which reflect the abundance of mRNAs coding for kainate and AMPA receptors, were similar. There was no difference in the sensitivity to kainate and in the voltage dependence of the kainate response. Responses mediated by NMDA, GABA, and glycine were unaffected by monocular enucleation. Sodium channel peak currents, activation, steady-state inactivation, and sensitivity to tetrodotoxin also remained unchanged after the enucleation. Our data show that mRNAs for major neurotransmitter receptors and ion channels in the adult rabbit visual cortex are not obviously modified by monocular deafferentiation. Thus, our results do not support the idea of a widespread dynamic modulation of mRNAs coding for receptors and ion channels by visual activity in the rabbit visual system.**

Neural plasticity, the property by which external events can change the functioning of the brain, is now known to occur in the *adult* visual system, even well after the critical period (for a review, see ref. 1). To a large extent, the molecular basis of activity-dependent changes in the adult visual system remains, at present, unknown. However, in the visual system of the adult monkey the absence of visual information from one eye leads to a drastic down-regulation of various molecules related to γ-aminobutyric acid (GABA)ergic and glutamatergic transmission in the regions formerly controlled by the impaired eye, as early as 1 week after the lesion (2–11). The modulation by visual activity of these molecules, notably neurotransmitter receptors and the mRNAs encoding them, could well be playing a crucial role in neural plasticity-related phenomena. For instance, activity-dependent changes in postsynaptic receptor densities could modulate synaptic strength in the visual system of adult animals (11).

To investigate this question in a broader context, we sought to study the regulation by visual activity of a wide variety of mRNAs coding for neurotransmitter receptors and ion channels in the adult visual cortex. To this end, we performed a monocular enucleation on adult rabbits. After 15 days, visual cortices on the same side as the lesion or on the opposite side were collected and mRNA was extracted from these regions. Because of the vast number of mRNAs that could be potentially modulated by visual activity, we used the *Xenopus* oocyte expression assay as a screening tool to determine which mRNAs coding for receptors and ion channels changed after monocular deafferentiation. We had shown previously that levels of mRNAs coding for several neurotransmitter receptors can be semiquantitatively estimated in visual structures by injecting whole mRNA from these areas into *Xenopus laevis* oocytes and assessing the level of expression of receptors by electrophysiological recordings (12). Using the same technique in this study, we were able to examine a large number of mRNAs from enucleated and control animals and were able to determine also some of the physiological and pharmacological properties of the receptors and channels expressed from these mRNAs.

We expected that the drastic lesion of monocular enucleation would induce, within reasonable time, large changes in the abundance of mRNAs. Because visual inputs are almost completely crossed in the rabbit (for instance, see ref. 13), differences in mRNA levels would be most pronounced between the visual cortex ipsilateral to the lesion (largely unaffected by the loss of visual inputs) and the one contralateral to the lesion (which receives the majority of its inputs from the enucleated eye). To our surprise, we were unable to demonstrate any clear change in the peak current or properties of kainate/α-amino-3-hydroxy-5-methylisoxazole-4-propionic acid (AMPA), *N*-methyl-D-aspartate (NMDA), GABA, or glycine receptors and voltage-activated sodium channels after monocular enucleation.

MATERIALS AND METHODS

Materials. Monocular deafferentiation was performed at the Universidad del Pais Vasco, Spain. Adult male pigmented Dutch-belted rabbits in the experimental group were anesthetized and underwent monocular enucleation under sterile conditions. The left eye was removed from the eye cup, and the animals were allowed to recover for 15 days in the Animal

Abbreviations: AMPA, α-amino-3-hydroxy-5-methylisoxazole-4-propionic acid; GABA, γ-aminobutyric acid; LCx, left cortex of monocularly enucleated animal; nLCx, left cortex of control animal; NMDA, *N*-methyl-D-aspartate; nRCx, right cortex of control animal; RCx, right cortex of enucleated animal; TTX, tetrodotoxin; vCx, visual cortex of control animal.

‡To whom reprint requests should be addressed. e-mail: rmiledi@uci.edu.

The publication costs of this article were defrayed in part by page charge payment. This article must therefore be hereby marked "*advertisement*" in accordance with 18 U.S.C. §1734 solely to indicate this fact.

Facility, after which their left and right visual cortices were collected. Proper care was given to minimize postoperative pain or discomfort. Visual cortices were dissected from enucleated and control, unoperated, rabbits as described earlier (12) and quickly frozen in liquid nitrogen.

mRNA Preparation and Injection. mRNA was prepared by the Chomczynski–Sacchi method (see ref.12 for a description of the procedure) and diluted to a concentration of 1 μg/μl. *Xenopus* oocyte harvesting, injection, and collagenase treatment have been described previously (14). Recordings started on day 4 after the injection until day 6–7.

Electrophysiological Recordings. mRNA-injected oocytes were placed in a recording chamber perfused with frog Ringer's solution (115 mM NaCl/2 mM KCl/1.8 mM $CaCl_2$/5 mM Hepes, pH 7.0), and the membrane potential was clamped either by an AxoClamp 2A (Axon Instruments, Foster City, CA), or an OC-725A oocyte clamp (Warner Instruments, Hamden, CT), usually at −60 mV. Drugs were delivered via a gravity-driven perfusion system. All membrane current measurements are given as mean ± SEM. Stimulation, recording of voltage-activated currents, I/V curves, and neurotransmitter responses, and analysis of data were performed by a suite of programs written for Microsoft Windows (15). In noise-analysis experiments, GABAergic currents were elicited by superfusion with GABA at concentrations well below the EC_{50}. Mean open time and conductance estimations were performed off-line with the SPAN program (courtesy of J. Dempster, University of Strathclyde, Glasgow, U.K.), following procedures described elsewhere (16). In some cases, the current variance did not give a reasonable value for the unitary current, especially at low GABA concentrations. The value for the unitary current was then taken from the power spectrum.

Voltage-activated sodium channels were elicited by clamping the cells at −100 mV and giving brief depolarizing pulses. The sensitivity to tetrodotoxin (TTX) was assessed by exposing oocytes to increasing concentrations of that drug (1–100 nM) for more than 1 min before giving the stimulation pulses. Leak and capacitive transients were removed by subtraction with records obtained in the presence of 313 nM TTX. At this concentration, sodium currents were no longer detectable.

Drugs. All drugs were from Sigma, except for AMPA, which was from Tocris-Cookson (Ballwin, MO).

RESULTS

mRNA preparations were obtained from the following: (*i*) The right visual cortices of monocularly enucleated animals, which received their input from the removed eye. These preparations will be referred to as RCx mRNAs. (*ii*) The left visual cortices of enucleated animals, ipsilateral to the lesion (LCx preparations). (*iii*) Control, normal rabbits. To exclude the possibility that mRNAs coding for receptors and channels might be asymmetrically distributed between left and right cortices, whole mRNA was extracted either from normal left cortices (nLCx preparations) or from normal right cortices (nRCx). In addition, mRNA was also prepared from both hemispheres of control visual cortices (vCx).

For simplicity, oocytes injected with RCx mRNA will be referred to as RCx oocytes, and oocytes injected with LCx mRNA will be called LCx oocytes, etc.

Kainate/AMPA Receptors. The application of 100 μM kainate to oocytes injected with mRNA from control or enucleated animals elicited smooth, large inward currents mediated by ionotropic kainate receptors (Fig. 1*A*). As shown in Fig. 1*B*, there was no substantial difference in the amplitude of responses between the cells injected with the different mRNAs, despite the lesion. AMPA, another agonist of ionotropic glutamate receptors, gave much smaller responses in all groups of cells. AMPA responses were, in average, 2.5%, 4.5%, 3.8%, and 3.5% of the kainate responses in nLCx, nRCx, LCx, and RCx oocytes, respectively. To assess whether monocular visual deprivation can change the properties of kainate receptors, we determined the dose–response relationship of kainate responses in nRCx, LCx, and RCx oocytes. All kainate responses, regardless of the lesion, had the same sensitivity to kainate, with an EC_{50} between 40 and 80 μM and a Hill coefficient close to 2, values that were identical to those we reported earlier (12). Likewise, kainate responses in oocytes injected with mRNA from control or enucleated animals displayed the same dependence on voltage, with a prominent inward rectification at potentials above −10 mV (Fig. 2).

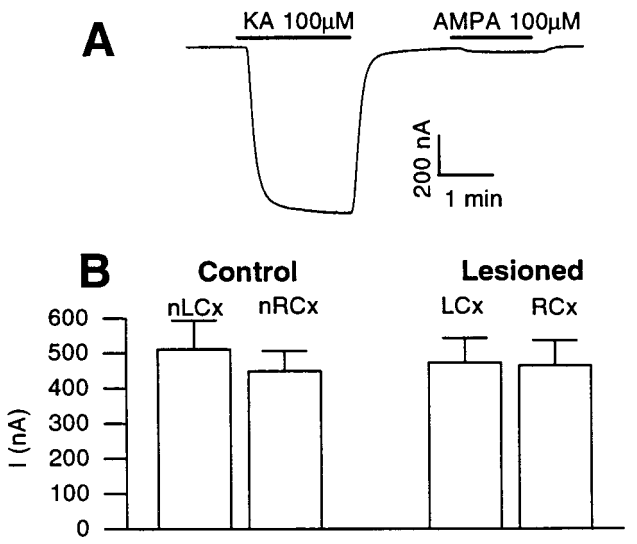

FIG. 1. (*A*) Kainate (KA) and AMPA responses in an oocyte injected with LCx mRNA (membrane potential: −60 mV). (*B*) Average amplitude (±SEM) of responses to 100 μM kainate (n = 22–28).

NMDA Receptors. As reported earlier (12), oocytes injected with mRNA from the rabbit visual cortex express functional NMDA receptors, which are activated by the coapplication of 100 μM aspartate and 100 μM glycine. Oocytes injected with mRNA from injured tissue gave small responses, not significantly different from those injected with mRNA from control tissue. The average currents were 33 ± 9 nA, 21 ± 6 nA, 16 ± 7 nA, and 21 ± 6 nA for nLCx, nRCx, LCx, and RCx oocytes, respectively.

GABA Receptors. All mRNA-injected oocytes elicited inward currents of variable amplitude on perfusion with 1 mM GABA. These responses were blocked by bicuculline (data not

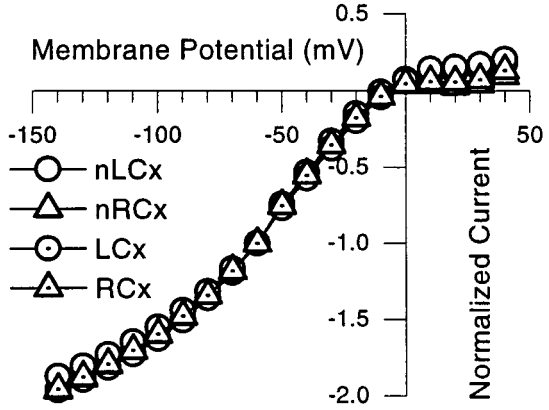

FIG. 2. I/V curves of kainate responses in nLCx, nRCx, LCx, and RCx oocytes. Kainate = 100 μM. Membrane currents at −60 mV were normalized to −1, and all other currents are reported relative to that value. Error bars have been removed for the sake of clarity.

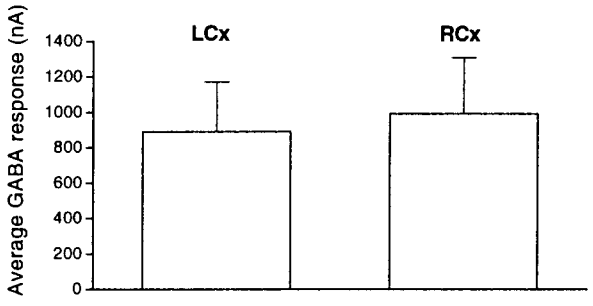

FIG. 3. Average GABA currents in oocytes injected with mRNA from the left or right visual cortices of enucleated animals (LCx and RCx oocytes, respectively; $n = 20–27$; -60 mV).

shown). Despite the variation in size of individual responses, there was no marked difference between the average GABA-elicited currents induced in oocytes injected with visual cortex mRNA from either the contralateral or the ipsilateral side of the lesion (Fig. 3) or from the right and left visual cortices of nonoperated animals (nLCx, 296 ± 62 nA; nRCx, 259 ± 55 nA).

GABA receptor desensitization was determined by fitting response decays immediately after the peak with the sum of two exponentials. Fitting parameters (residual amplitude A_∞, amplitudes of the two components A_1 and A_2, and time constants τ_1 and τ_2) are summarized in Table 1. In essence, these values indicate that the desensitization rate of GABA receptors expressed in oocytes is not altered by monocular enucleation.

Sensitivity to GABA was summarily studied in two oocytes injected with mRNA from the right visual cortex of enucleated animals, the side that would have been affected the most by the lesion. Dose–responses were in all respects similar to the ones reported earlier with rat cortex (14), with an EC_{50} around 50 μM and a Hill coefficient of 1.6.

To assess whether monocular enucleation affects the single-channel properties of GABA receptors, we determined the mean open time and unitary conductance of GABA receptors expressed in vCx, LCx, and RCx oocytes by stationary noise analysis (16–18). The values for the unitary conductance, calculated either from the current variance or from the asymptotic value at $f = 0$ Hz in the power density spectrum, are shown in Table 2. Assuming a reversal potential for chloride of -20 mV (19), our estimates point to a conductance of 23–26 pS for GABA receptors expressed in all groups of oocytes. Current power density spectra were well fitted with the sum of two Lorentzians, one of which had a very low corner frequency. Because this component is variable (20), we derived the mean open time from the corner frequency of the other Lorentzian. In all oocytes, this value gave an estimate of the mean open time close to 10 ms (see Table 2).

Glycine Receptors. Inhibitory glycine receptors were expressed at low levels in all groups of oocytes, with no change in the glycine response in oocytes injected with mRNA from the lesion side versus cells injected with mRNA from the nonlesion side. Activation of these receptors by 1 mM glycine led to average currents of 6 ± 1.6 nA (nLCx) and 4 ± 0.6 nA (nRCx) in oocytes injected with control mRNA and 17 ± 5.6 nA versus 15 ± 4.2 nA in oocytes injected with LCx and RCx mRNA, respectively.

Table 1. Desensitization of the GABA response in visual cortex oocytes, expressed in terms of the decay curve normalized response $= A_\infty + A_1 e^{-t/\tau_1} + A_2 e^{-t/\tau_2}$

Exponential fitting parameters	vCx (Control)	LCx (Enucleated)	RCx (Enucleated)
A_∞, % max response	6.5 ± 2.6	7.7 ± 2.0	9.5 ± 1.6
A_1, % max response	52.8 ± 24.6	52.9 ± 23.1	43.2 ± 11.9
A_2, % max response	40.7 ± 25.4	42.0 ± 21.6	48.9 ± 10.9
τ_1, s	24.0 ± 5.8	33.0 ± 6.0	19.0 ± 2
τ_2, s	61.0 ± 7.15	90.0 ± 17	65.0 ± 8.5

GABA = 1 mM. Values are given as mean ± SEM.

Table 2. Unitary conductance and mean open time of GABA receptor channels expressed in oocytes injected with visual cortex mRNA

Unitary conductance parameters	vCx (Control)	LCx (Enucleated)	RCx (Enucleated)
γ, pS	23.6 ± 3.95	25.2 ± 3.14	25.8 ± 3.26
τ, ms	9.2 ± 1.16	11.55 ± 1.90	9.84 ± 1.24

GABA = 3–10 μM. Values are given as mean ± SEM.

Voltage-Activated Sodium Channels. In virtually all mRNA-injected oocytes, depolarization from a holding potential of -100 mV to voltages above -20 mV activated large TTX-sensitive sodium currents.

Current Amplitudes. Peak sodium currents were registered at -10 mV and consisted of an inward, fast decaying, TTX-sensitive current (Fig. 4*A*). Average peak amplitudes in nLCx, nRCx, LCx, and RCx oocytes are given in Fig. 4*B*. As in the case with neurotransmitter receptors, enucleation does not dramatically change the expression of sodium channels in oocytes injected with visual cortex mRNA.

Activation. In all oocytes, 50-ms depolarizing pulses from -100 mV started to activate sodium currents at around -40 mV. These reached a peak at potentials close to -10 mV, and became smaller at higher potentials. Normalized I/V curves do not show any shift in activation associated with enucleation and are, for all practical purposes, similar in all groups of oocytes (Fig. 5).

Steady-State Inactivation. Steady-state inactivation was determined in each group of oocytes by a standard two-pulse protocol, in which a 100-ms prepulse, ranging from -100 mV to 0 mV, preceded a 20-ms test pulse at -10 mV. The *Inset* of Fig. 6 illustrates the inactivation of sodium channels in visual cortex oocytes, while the main graph is a plot of h_∞ (the ratio between the test current at a particular prepulse potential and the largest test current) versus the prepulse potential for each group of oocytes. Irrespective of the lesion, all curves are quite similar, and they can be approximated with a two-state Boltzmann equation of the form $h_\infty = 1/\{1 + \exp[(V - V_{1/2})/n]\}$,

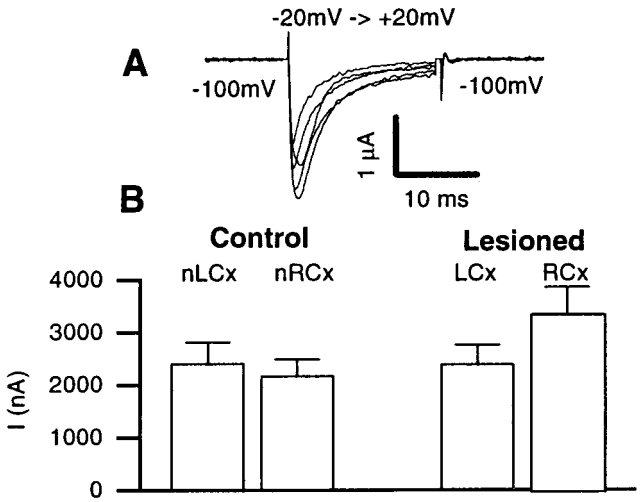

FIG. 4. (*A*) Activation of voltage-activated sodium channels in a RCx oocyte. Sodium currents were elicited by giving voltage pulses from -20 mV to $+20$ mV in 10-mV increments. Leak and capacitive currents were removed off-line by TTX subtraction. (*B*) Means (±SEM) of peak sodium currents in oocytes injected with nLCx, nRCx, LCx, and RCx mRNA ($n = 22–28$).

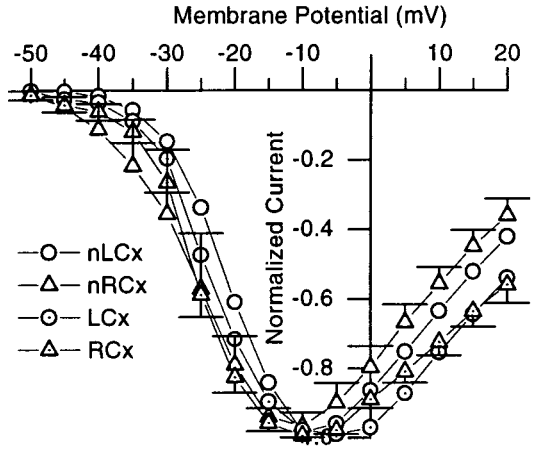

FIG. 5. Activation curves for sodium currents in oocytes injected with nLCx, nRCx, LCx, or RCx mRNA. Currents for each oocyte were normalized relative to the largest current within the range tested. Each point and error bar represent the mean of normalized currents ± SEM.

where n is the slope ratio and $V_{1/2}$ is the half-maximal voltage. Fitting these curves gave a slope ratio close to 7 and a $V_{1/2}$ of −38 mV.

TTX Sensitivity. TTX between 1 and 100 nM inhibited voltage-activated sodium channels expressed from visual cortex mRNA in a dose-dependent manner. Peak current attenuation curves (Fig. 7) were identical in all oocytes, indicating that enucleation does not induce the expression of TTX-insensitive sodium channels in visual cortex oocytes. A concentration of 7–9 nM TTX was sufficient to inhibit sodium currents by half. Furthermore, these curves can be well fitted by a Langmuir absorption isotherm with a Hill coefficient of 1–1.3 and a K_d of 9 nM, suggesting, that, in visual cortex oocytes, one molecule of TTX is sufficient to block one sodium channel. The TTX block was not voltage dependent, as a given concentration of TTX would produce the same attenuation whether at −20, −10, 0, or +10 mV (data not shown). At 313 nM TTX, there was no evidence for any residual voltage-activated current.

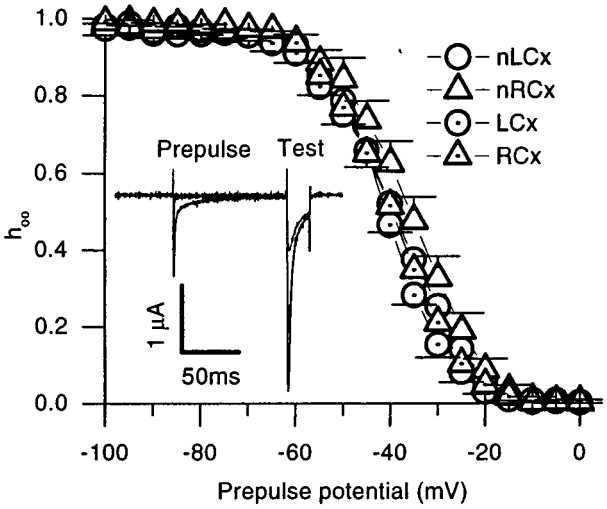

FIG. 6. h_∞ ratio versus potential. Each point is the mean (±SEM) of the ratio between the amplitude of the test current at a given potential and the largest test current. For the sake of clarity, error bars are not shown. (*Inset*) Steady-state inactivation of sodium currents in an oocyte injected with RCx mRNA. Shown here are superimposed records with prepulse voltages ranging from −50 mV to −30 mV. Leak and capacitive currents were removed by TTX subtraction.

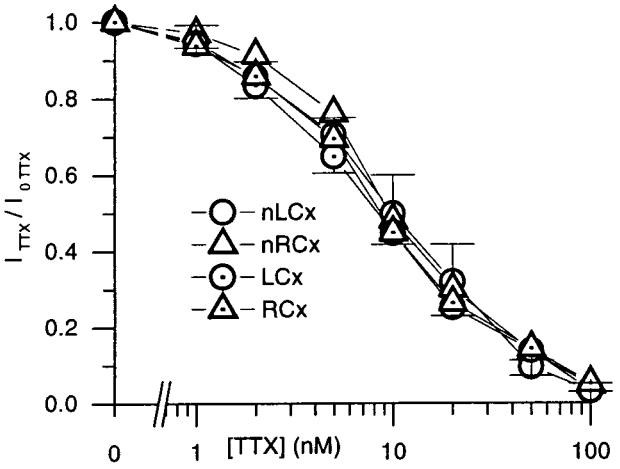

FIG. 7. Inhibition of sodium currents by TTX in visual cortex oocytes. Averages of normalized currents. For the sake of clarity, error bars are not shown.

DISCUSSION AND CONCLUSION

Our results provide compelling evidence that monocular enucleation in the adult rabbit does not significantly change the level of mRNAs coding for kainate/AMPA, NMDA, GABA, or glycine receptors and voltage-activated sodium channels. Moreover, the lesion has no effect on the main pharmacological and electrophysiological properties of these receptors and channels. Noticeable changes in current amplitude, time-course, or pharmacological properties of the responses in mRNA-injected oocytes would have reflected, in a semiquantitative manner, significant differences in the amount or nature of the mRNAs from the visual cortices of enucleated and control animals. Although the technique used does not give an absolute measure of mRNAs (as with Northern blots), and does not provide information about their localization (contrary to *in situ* hybridization, for instance), the *Xenopus* expression system does not require a prior knowledge of the sequence of the mRNAs studied and can be used as an assay to rapidly assess the amount of mRNAs in various brain regions (12). A great many receptors and ion channels expressed in mRNA-injected oocytes are functional with properties that closely mimic those found in native tissues. In that respect, the oocyte expression system is particularly well adapted to detect subtle functional changes in receptor properties due to the developmental maturation of receptors (see, for instance, ref. 21) or to artificial mutations (e.g., ref. 22). Therefore, our failure to see any significant changes after enucleation cannot be entirely attributed to the technique we used. In addition, our experiments were designed to maximize the effects of the lesion. We assumed that changes brought about by monocular deafferentiation in rabbits would be even stronger than in monkeys, considering that the visual system of the rabbit is almost entirely lateralized, as 85% of the fibers from one eye project exclusively to the contralateral visual structures (13). Furthermore, the time between enucleation and cortex removal was well within the time frame during which changes were seen in monkeys (for instance, see ref. 8). Finally, the method we used, which consisted of enucleating the eye, left no doubt that all visual inputs from the eye were effectively removed.

Modulation of specific mRNAs by cellular activity has long been proposed as a general mechanism to modify receptor levels (for a review, see ref. 23). Such changes are exemplified at the denervated neuromuscular junction, where denervation supersensitivity (24, 25) is accompanied by an *increase* in the level of mRNAs coding for acetylcholine nicotinic receptors (for a review, see ref. 26). Up-regulation of receptor mRNAs

after denervation has also been observed in the central nervous system. For instance, deafferentiation of the striatum by creating a lesion in the nigrostriatal pathway leads to an increase in the level of mRNA coding for dopamine D2 receptors (27). In other systems, deafferentiation leads to a *decrease* in the level of existing mRNAs. This was observed in the visual cortex of monocularly deprived adult monkeys as early as 1 week post-lesion (8). In addition, denervation could induce the appearance of mRNA molecules coding for new subunits. These subunits may not exist prior to the lesion in the adult, but are present only in the newborn animal, as is the case for the δ subunit of the muscular nicotinic receptor (26). In the light of these findings pointing to a widespread range of responses that various tissues exhibit after denervation, it is surprising that we could not detect any significant changes after monocular enucleation. Because response amplitudes in "visual cortex" oocytes are not dramatically enhanced or reduced by the lesion, there is no reason to support the idea that monocular enucleation increases levels of mRNAs coding for excitatory and inhibitory amino-acid receptors and voltage-gated sodium channels in the adult rabbit visual cortex.

Excitatory Amino-Acid Receptors. On the basis of our data, there is little support for a denervation supersensitivity-like phenomenon for kainate/AMPA receptors. This is even more unexpected when considering that, in the monkey, monocular lesion reduces the level of glutamate in the ocular dominance columns controlled by the eye with the lesion (10). Such a decrease in neurotransmitter levels in the rabbit visual cortex would have favored, in theory, an *increase* in the abundance of mRNAs coding for kainate/AMPA receptors. We also hypothesized that, because the neuromuscular junction seems to revert to a neonatal stage after denervation (28), the adult rabbit visual cortex might react in a similar way, by increasing the expression of neonatal mRNAs after monocular deprivation. We were particularly interested in the response to AMPA relative to kainate, as the ratio AMPA response/kainate response is higher in the neonatal brain (Q.-T.N. and R.M., unpublished observations). However, it is clear that monocular deafferentiation does not affect this value.

Inhibitory Amino-Acid Receptors. Similarly, we looked at the expression of inhibitory glycine receptors, because, in the newborn, mRNA molecules coding for glycine receptors are present at much higher levels than in the adult brain (29). Our results show that monocular enucleation does not increase the expression of glycine receptors in the visual cortex innervated by the eye with the lesion.

One of the most salient results of our study is the absence of GABA receptor mRNA down-regulation, contrary to results previously reported for monkeys (8). Because our assessment of GABA receptor mRNA levels is based on the measurement of GABA-elicited currents, a decrease in the number of receptors expressed in oocytes (resulting from a lower level of mRNA coding for GABA receptors resulting from the lesion) could have been masked by an increase in the conductance or in the mean open time of the channels associated with GABA receptors. However, our results with noise analysis show that the lesion does not affect the electrophysiological properties of the GABA receptors expressed in oocytes. Therefore, our results show that mRNAs coding for GABA receptors remain largely unaffected by monocular enucleation.

Sodium Channels. Denervation of adult striatal muscles induces the overexpression of voltage-activated sodium channels, as well as the appearance of TTX-insensitive sodium channels (30). Our results indicate that none of these phenomena seem to occur after monocular deafferentiation in the adult visual cortex. Functional expression of cloned sodium channels in oocytes has highlighted the role of the β1 auxiliary subunit in the response amplitude and in other physiological characteristics such as activation and steady-state inactivation (31). Because there are no obvious differences between the activation and steady-state inactivation curves among all groups of oocytes, it is very unlikely that monocular enucleation decreases levels of the β1 subunit in the adult rabbit visual cortex.

Altogether, our results do not support the notion that a dynamic modulation of mRNAs coding for neurotransmitter receptors and voltage-activated sodium channels by visual activity is a widespread mechanism used in the visual cortex to deal with drastic changes in sensory stimuli. The fact that our data were not expected, especially in the light of the findings regarding GABA receptor mRNAs in monkeys (8), leads us to think that there is a fundamental difference between mammals such as monkeys and rabbits, in the way their visual system reacts after drastic changes in visual input. Our view is supported by the fact that cortical reorganization in the adult does not always happen after monocular enucleation and could be highly dependent on the cytoarchitecture of the visual cortex. For instance, in the rabbit, monocular enucleation fails to induce a functional reorganization of the visual cortex (32). Even in the adult cat, in which retinal lesions are known to modify visual maps in the cortex, monocular inactivation does not shift the receptive field of most cells in the peripheral representation of visual area V1 (33). In conclusion, we speculate that, at the molecular level, modulation of mRNAs by visual activity parallels functional changes in receptive fields at the cellular level. The fact that these molecular and cellular changes do not occur in adult rabbits challenges our current opinion that the visual cortex is, across species, capable of extensively reorganizing itself even well after birth.

We thank Dr. David J. Fogarty (Universidad del Paris Vasco) and Prof. S. Zeki (University College, London) for their useful comments on the manuscript. This work was supported by a grant from the National Institute of Neurological Disorders and Stroke (DNS 23284-09).

1. Kaas, J. H. (1991) *Annu. Rev. Neurosci.* **14,** 137–167.
2. Hendry, S. H. & Jones, E. G. (1986) *Nature (London)* **320,** 750–753.
3. Hendry, S. H. & Jones, E. G. (1988) *Neuron* **8,** 701–712.
4. Hendry, S. H., Fuchs, J., de Blas, A. L. & Jones, E. G. (1990) *Prog. Brain Res.* **90,** 497–502.
5. Benson, D. L., Isackson, P. J., Hendry, S. H. & Jones, E. G. (1989) *Brain Res. Mol. Brain Res.* **5,** 279–287.
6. Jones, E. G., Benson, D. L., Hendry, S. H. C. & Isackson, P. J. (1990) *Cold Spring Harbor Symp. Quant. Biol.* **55,** 481–490.
7. Hendry, S. H., Huntsman, M. M., Vinuela, A., Mohler, H., de Blas, A. L. & Jones, E. G. (1994) *J. Neurosci.* **14,** 2383–2401.
8. Huntsman, M. M., Isackson, P. J. & Jones, E. G. (1994) *J. Neurosci.* **14,** 2236–2259.
9. Huntsman, M. M., Leggio, M. G. & Jones, E. G. (1995) *J. Comp. Neurol.* **352,** 235–247.
10. Carder, R. K. & Hendry, S. H. (1994) *J. Neurosci.* **14,** 242–262.
11. Hendry, S. H. & Miller, K. L. (1996) *Visual Neurosci.* **13,** 223–235.
12. Matute, C., Nguyen, Q.-T. & Miledi, R. (1993) *J. Neurosci. Res.* **35,** 652–663.
13. Granit, R. (1962) in *The Eye*, ed. Dawson, H. (Academic, New York), pp. 541–548.
14. Polenzani, L., Woodward, R. M. & Miledi, R. (1991) *Proc. Natl. Acad. Sci. USA* **88,** 4318–4322.
15. Nguyen, Q.-T. & Miledi, R. (1995) *J. Neurosci. Methods* **61,** 213–219.
16. Morales, A., Nguyen, Q.-T. & Miledi, R. (1994) *Proc. Natl. Acad. Sci. USA* **91,** 3097–3101.
17. Anderson, C. R. & Stevens, C. F. (1973) *J. Physiol. (London)* **235,** 655–691.
18. Katz, B. & Miledi, R. (1972) *J. Physiol. (London)* **224,** 665–699.
19. Kusano, K., Miledi, R. & Stinnakre, K. (1982) *J. Physiol. (London)* **328,** 143–179.
20. Miledi, R., Parker, I & Sumikawa, K. (1982) *EMBO J.* **1,** 1307–1312.
21. Akagi, H. & Miledi, R. (1988) *Science* **242,** 270–274.
22. Palma, E., Eusebi, F. & Miledi, R. (1997) *Proc. Natl. Acad. Sci. USA* **94,** 1539–1543.

23. Morris, B. J. (1993) *Mol. Neurobiol.* **7,** 189–205.
24. Axelsson, J. & Thesleff, F. (1959) *J. Physiol. (London)* **147,** 178–193.
25. Miledi, R. (1960) *J. Physiol. (London)* **151,** 1–23.
26. Laufer, R. & Changeux, J.-P. (1989) *Mol. Neurobiol.* **3,** 1–53.
27. Neve, K. A., Neve, R. L., Fidel, S., Janowsky, A. & Higgins, G. A. (1991) *Proc. Natl. Acad. Sci. USA* **88,** 2802–2806.
28. Diamond, J. & Miledi, R. (1962) *J. Physiol. (London)* **162,** 393–408.
29. Carpenter, M. K., Parker, I & Miledi, R. (1988) *Proc. R. Soc. London Ser. B* **234,** 159–170.
30. Redfern, P. & Thesleff, S. (1971) *Acta Physiol. Scand.* **82,** 70–78.
31. Isom, L. L., De Jongh, K. S., Patton, D. E., Reber, B. F., Offord, J., Charbonneau, H., Walsh, K., Goldin, A. L. & Catterall, W. A. (1992) *Science* **256,** 839–842.
32. Clarke, R. J., Datskovski, B. W., Grigonis, A. M. & Murphy, E. H. (1992) *Exp. Brain Res.* **91,** 303–310.
33. Rosa, M. G. P., Schmid, L. M. & Calford, M. B. (1995) *J. Physiol. (London)* **482,** 589–608.